Structure of neutron-rich Ar isotopes beyond N=28

S. Bhattacharyya, M. Rejmund, A. Navin, E. Caurier, F. Nowacki, A. Poves, R. Chapman, D. O'Donnell, M. Gélin, A. Hodsdon, et al.

Structure of neutron-rich Ar isotopes beyond N=28

S. Bhattacharyya,[1,*] M. Rejmund,[1] A. Navin,[1,†] E. Caurier,[2] F. Nowacki,[2] A. Poves,[3]
R. Chapman,[4] D. O'Donnell,[4] M. Gelin,[1] A. Hodsdon,[4] X. Liang,[4] W. Mittig,[1] G. Mukherjee,[1,*]
F. Rejmund,[1] M. Rousseau,[2] P. Roussel-Chomaz,[1] K-M. Spohr,[4] and Ch. Theisen[5]

[1]*GANIL, CEA/DSM - CNRS/IN2P3, Bd Henri Becquerel, BP 55027, F-14076 Caen Cedex 5, France*
[2]*IPHC, UMR7178, IN2P3-CNRS et Université Louis Pasteur, BP28, F-67037 Strasbourg, France*
[3]*Departamento de Fisica Teorica and IFT/CSIC,*
Universidad Autonoma de Madrid, 28049 Madrid, Spain
[4]*School of Engineering and Science, University of the West of Scotland, PA1 2BE Paisley, Scotland, United Kingdom*
[5]*CEA-Saclay DSM/DAPNIA/SPhN, F-91191 Gif/Yvette Cedex, France*

(Dated: June 25, 2008)

Results from the gamma spectroscopy of ^{47,48}Ar exemplifying new limits of sensitivity for characterizing neutron-rich nuclei at energies around the Coulomb barrier are presented. The present results along with interacting shell model calculations, highlight the role of cross shell excitations and indicate the presence of a non axial deformation in ^{48}Ar.

PACS numbers: 21.60.Cs, 23.20.Lv, 27.40.+z, 25.70.Lm

The availability of rare isotopic beams has opened up new avenues to study the evolution of nuclear structure as a function of neutron-proton asymmetry in addition to the earlier studied degrees of freedom, namely temperature and angular momentum. The appearance/disappearance of closed shell configurations at extreme values of isospin has attracted a lot of attention. The quest towards the understanding of how and if atomic nuclei near closed shells develop collective excitations/deformation with the available limited single-particle degrees of freedom is also of current interest. Advances in experimental techniques, especially with in-beam γ -ray spectroscopy, now allow us to probe nuclei having twice the number of neutrons as protons. They provide an opportunity not only to search for "islands of inversion" but also for nuclei that are deformed near a spherical shell closures [1, 2]. The deviation from the spherical symmetry (β) and the axial symmetry (γ) are often used to characterize nuclear shapes. Nuclei near "conventional" closed shells at extremes of isospin, thus, could offer a new domain for the study of the role of neutron-proton correlations on collective motion. This could be a fertile region to search for nuclei that violate axial symmetry (first discussed by Davydov and collaborators [3] half a century ago) complementing those made at high angular momentum.

In isotopes (isotones) spanning neutron (proton) numbers around the $N(Z) = 20,\ 28$ shell gaps, the couplings and/or the excitations of valence nucleons across a shell play a key role in determining the excitation spectra [4]. The nuclei in this region have been reported to show a wide variety of shapes, including evidence for shape coexistence [5, 6] and superdeformation [7]. Shell model calculations have kept pace with experimental developments both to predict and understand the evolution of such structure away from stability. The *sdfp* effective interaction [8], among others, has been successfully used to explain regions of deformation like that observed in ^{42}Si$_{28}$ [1, 9], the neutron-rich Sulphur isotopes [5, 6] and the evolution of the spin-orbit splitting around $N = 28$ [10]. The present work, in addition to increasing our understanding of cross-shell excitations around the double "magic" ^{48}Ca, is motivated by the search and understanding of the existence of nuclei having a triaxial ellipsoid shapes in this region [11].

Deep inelastic transfer reactions made at energies near the Coulomb barrier have shown to be an efficient way to study neutron-rich nuclei both with sufficient excitation and angular momentum [12, 13]. This technique is complementary to spectroscopy using fast fragmentation beams. Nuclei that have no known spectroscopic information need to be uniquely identified, for example by a spectrometer [1, 2, 14], before any transitions can be assigned. In the present work a 1.310 GeV ^{238}U beam, with an intensity of ~ 2 pnA, from the GANIL cyclotron facility was used on an isotopically enriched ^{48}Ca target (thickness 1 mg/cm^2) to produce neutron-rich nuclei around ^{48}Ca using deep inelastic transfer reactions. These measurements utilize the advantages of inverse kinematics (higher recoil energies and kinematic focusing of the residues). The large acceptance variable mode spectrometer (VAMOS), placed at 35° with respect to the beam axis, was used to identify the target-like residues. The focal plane detection system consisted of two position sensitive drift chambers separated by a distance of one meter, one Secondary Electron Detector (SeD), placed between the two drift chambers, a segmented ionization chamber and a 21-element Si-wall [13, 14]. The Z identification was obtained from the energy loss measured in the ionization chamber and the residual energy in the Si-wall. The time of flight of the recoils was measured by the SeD, relative to the radio frequency of the cyclotron and was used to obtain the velocity. The measured parameters at the focal plane along with the known mag-

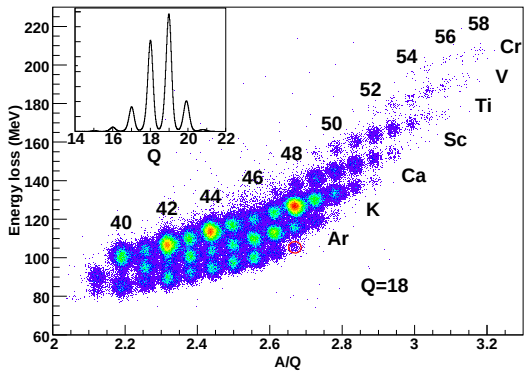

FIG. 1: (color online) Energy loss measured in the ion chamber as a function of the derived mass/charge (A/Q) for a selected charge state $Q = 18$. The inset shows the charge state distribution, obtained from the derived A and A/Q.

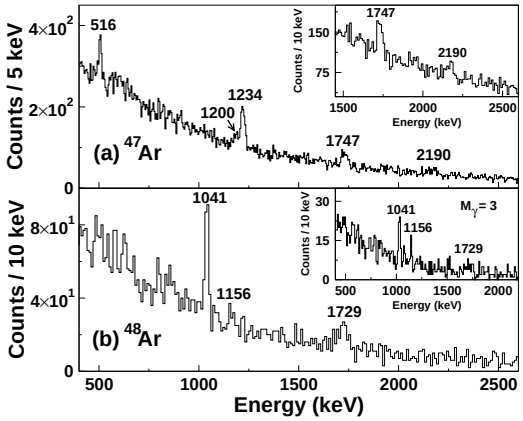

FIG. 2: Doppler corrected γ spectra for the Ar isotopes obtained in coincidence with corresponding residues detected. (a) ^{47}Ar. The inset shows an expanded view of the high energy region of ^{47}Ar spectrum. (b) ^{48}Ar. The inset shows the spectrum when at least 3 clover detectors have fired.

netic field were used to reconstruct the magnetic rigidity, the mass (A), mass/charge (A/Q), the scattering angle after the reaction and the path length on an event by event basis. The final selection of a particular nucleus was made from a two dimensional identification matrix of energy loss vs. A/Q for each charge state. Figure 1 shows a typical plot obtained for a single Si detector for a charge selection of $Q = 18$, where the unique identification of the various nuclei ($Z \geq 18$) can be clearly seen. The Doppler corrected γ-ray spectra, in coincidence with the fragments, were obtained using the EXOGAM array, consisting of 11 segmented clover detectors, placed at a distance of 11.4 cm around the target in a closed-pack configuration with partial Compton suppression. The angle between the γ-ray (from the segment of the relevant clover detector) and the reconstructed velocity vector of the emitting target-like nucleus (obtained from the measurements in the VAMOS spectrometer) were used to obtain the γ-ray energy in the rest frame. A typical energy resolution obtained is about 20 keV at 1 MeV. Figure 2 shows the Doppler corrected spectra for the ^{47,48}Ar isotopes. It should be pointed out that in such exotic nuclei the use of $\gamma-\gamma$ coincidences to generate the level scheme is presently not possible. Further experimental details can be found in Ref. [14].

Gaudefroy *et al.* [10] reported the excitation energies and spectroscopic factors through the d(^{46}Ar,^{47} Ar)p reactions for states in ^{47}Ar. Different states can be expected to be populated in the present work due to the selectivity of the reaction mechanism. The γ-ray spectrum in coincidence with ^{47}Ar fragments shown in Fig. 2a is reported for the first time. The level scheme shown in Fig. 3a was constructed based on an intensity balance of the γ rays and also from a comparison with the level structure reported in Ref. [10]. The 1200(6) and the 1747(5) keV states correspond to the 1130(75) and 1740(95) keV levels reported earlier. The new transitions 516(4), 1234(4) and 2190(16) keV in addition to the 1200 and 1747 keV transitions can also be seen in the figure. The position of the 2190 keV level is tentative and is based on a relatively large decrease in the yield for a higher clover fold selection.

The present experiment also reports for the first time the γ-ray spectroscopy of ^{48}Ar. This to the best of our knowledge represents the spectroscopy of the highest N/Z nucleus obtained using stable beams around the Coulomb barrier. Only a report on the lifetime [15] of the ground state exists in literature. The assignment of the γ-rays was possible due to an unambiguous identification of the coincident ^{48}Ar fragments in VAMOS. The corresponding Doppler corrected γ ray spectrum is shown in Fig. 2b. Three γ-rays are clearly visible in the spectra, namely 1041(9) keV, 1156(15) keV and 1729(13) keV. The corresponding level scheme shown in Fig. 3a was obtained using an intensity balance and using a fold selection of the clover detectors. The relatively large population of non-yrast states in addition to yrast states has been shown in deep inelastic reactions [13]. This was further verified in the Ar isotopes especially in ^{40}Ar where even the population of the 2_3^+ was observed rather than the population of a 6^+ state. This aspect of the reaction mechanism was further used to constrain the proposed level scheme, especially the tentative assignment of the 2_2^+ state at 2197 keV. Fig. 3b shows the systematics for the energies of the first 2^+ and 4^+ states as a function of the neutron number for even-even isotopes of Ar. Data are taken from Ref. [16]. The energy and proposed assignment of the low-lying states in ^{48}Ar appear to consistent with the tentative assignments of the known 2^+ and 4^+ levels of the Ar isotopes.

The theoretical interpretation of the measured levels was carried out within an Interacting Shell Model (ISM)

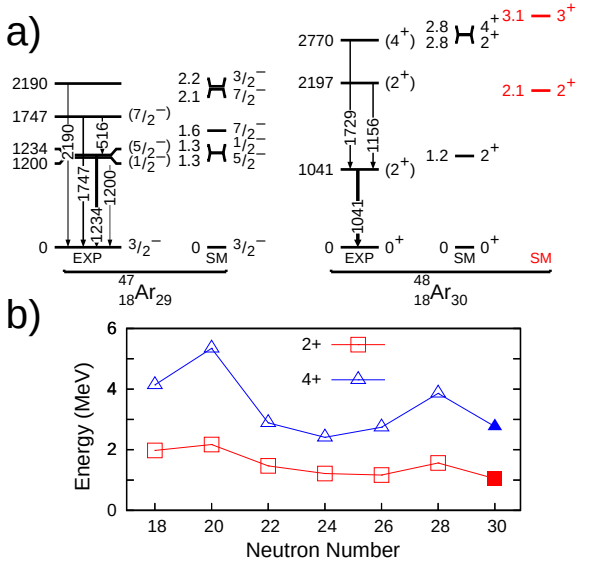

FIG. 3: (color online) a) Level schemes of ^{47,48}Ar (EXP) obtained in the present work and results of interacting shell model calculations (SM) (see text). The electromagnetic transitions are indicated by arrows; the widths indicate their relative intensities. b) The energies of the first 2^+ (squares) and 4^+ (triangles) states in the isotopes of Argon as a function of neutron number. Data are from [16]. The filled symbols are from the present work.

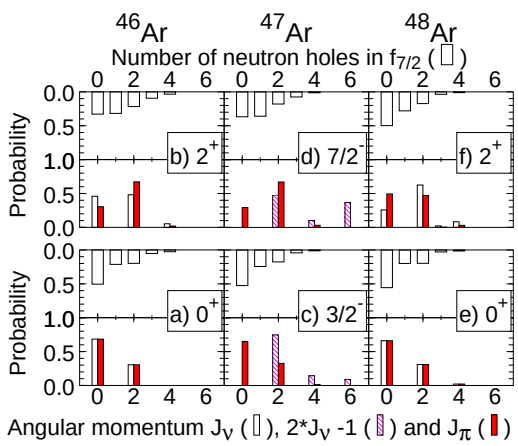

FIG. 4: (color online) Calculated shell model probabilities for $^{46-48}$Ar as a function of the angular momentum of the neutrons (ν) and protons (π) space (bottom panel) and the number of neutron holes in the $\nu 0f_{\frac{7}{2}}$ (top panel). In the case of ^{47}Ar due to the presence of an unpaired neutron, the angular momentum is represented as $2 * J_\nu - 1$.

framework using the code NATHAN [17]. The interaction employed includes a recent improvement [18] of the *sdfp* interaction [8]. The valence space consists of the *sd*-shell for protons and the *pf*-shell for neutrons without any restrictions. We also discuss the signatures of triaxiality following the prescription of Davydov and Filippov [3] within this model. The comparison of the experimental level schemes with the results of the shell model calculations is shown in Fig. 3a. There is a very good agreement between experimental and calculated states. The low lying states of ^{47}Ar can be easily interpreted with the help of the ISM calculations. The ground state $\frac{3}{2}^-$ and the excited $\frac{1}{2}^-$ state correspond respectively to the coupling of a $1p_{\frac{3}{2}}$ and a $1p_{\frac{1}{2}}$ neutron to the highly correlated 0^+ ground state of ^{46}Ar. On the contrary, the doublet $\frac{5}{2}^-$, $\frac{7}{2}^-$ results from the coupling of a $1p_{\frac{3}{2}}$ neutron to the 2^+ state of ^{46}Ar. The calculated ratio of the intensities for the decay of $\frac{7}{2}^-$ state to the $\frac{5}{2}^-$ (M1+E2) and $\frac{3}{2}^-$ (E2) is 0.3 which compares well to the experimental ratio of 0.8(3).

In ^{48}Ar, the data show a strong branch from the 2_2^+ state to the 2_1^+ relative to the direct decay to the 0^+ ground state. The intensity limit for the latter was found to be $< 30\%$ of that observed for the $2_2^+ \rightarrow 2_1^+$ transition. The inset of Fig. 2b points towards a peak-like structure at around 1085 keV, which could be a candidate for a transition between the 3^+ and 2_2^+ states. The ratio of the experimental energies $E(2_2^+)/E(2_1^+)$, $E(4_1^+)/E(2_1^+)$ are consistent with a signature of triaxiality as given in Ref. [3]. These experimental observations combined with the appearance of a low lying 3^+ state in the ISM results (Fig. 3a) strengthen the hypothesis of ^{48}Ar being triaxial. Further and more importantly, the calculated $B(E2)(3_1^+ \rightarrow 2_1^+)$ in ^{48}Ar is an order of magnitude smaller than the $B(E2)(3_1^+ \rightarrow 2_2^+)$ and the $B(E2)(2_2^+ \rightarrow 0_1^+)$ is also an order of magnitude smaller than the $B(E2)(2_2^+ \rightarrow 2_1^+)$. In the $\gamma = 30°$ case, the $B(E2)(2_2^+ \rightarrow 0_1^+)$ is strictly zero, and in the $\gamma = 0°$ (prolate) or $\gamma = 60°$ (oblate) case it is the $B(E2)(2_2^+ \rightarrow 2_1^+)$ which is strictly zero.

These signatures of collectivity can be also explained by analyzing the properties of the calculated states in terms of (i) the individual angular momentum of neutrons (J_ν) and protons (J_π) coupled to form an observable final state J with $|J_\nu \otimes J_\pi, J\rangle$ and (ii) the number of the neutron particle-hole (N_{ph}) excitations across the $N = 28$ shell gap (equivalent to the number of holes in the $\nu 0f_{\frac{7}{2}}$ orbital). Such an approach provides a greater physical insight into excitations in these nuclei. Fig. 4 shows the calculated shell model probabilities for the ground and excited states in $^{46-48}$Ar. The bottom panel shows them as a function of the decomposition in terms of individual neutron (J_ν) and proton (J_π) angular momenta. The corresponding top panel shows them as function of the number of neutron(s) promoted out of the $\nu 0f_{\frac{7}{2}}$ orbital. As can be seen from the top panel of Fig. 4(a,e) the ground states of the even isotopes of Ar, are described as having only $\sim 50\%$ of a $N = 28$ closed shell configuration. The corresponding $N = 28$ closed core configuration for ^{48}Ca is $\sim 90\%$ [4]. References [4, 18, 19] discussed some aspects of the excitation in terms of N_{ph}

excitations and Ref. [10] indicated that the $N = 28$ is not fully closed in ^{46}Ar. The remaining part of the wavefunction of the 0^+ states in ^{46,48}Ar is almost equally shared between one and two neutron excitations ($N_{ph} = 1, 2$) across the $N = 28$ gap. The remarkably large contribution of the $J_\nu = J_\pi = 2$ excitations ($\sim$ 30%) in the 0^+ ground states of ^{46,48}Ar can be seen from the corresponding bottom panels. Fig. 4(b,f) show that the 2^+_1 states are a mixture of both neutron ($J_\nu = 2$) and proton ($J_\pi = 2$) states. The reason that the $N_{ph} = 0$ in the 2^+_1 state of ^{46}Ar is smaller than the corresponding ^{48}Ar value is because, in order to make a 2^+ neutron state in ^{46}Ar it is necessary to open the $0f_{\frac{7}{2}}$ closed neutron orbit, which is not the case for ^{48}Ar. Fig. 4(c,d) quantifies the nature of the states in ^{47}Ar, discussed earlier, namely that the ground state can be represented as a coupling of the 0^+ state of ^{46}Ar to a $\nu 1p_{\frac{3}{2}}$ neutron. The first $\frac{7}{2}^-$ state can be seen to have a dominant contribution arising from the coupling of 2^+ state of ^{46}Ar and a $\nu 1p_{\frac{3}{2}}$ neutron.

The shell model calculations discussed above thus predict that beyond $N = 28$, the neutron rich isotopes of Argon still have large probability of excitation of one or two neutrons across the $N = 28$ gap. The implications of the large fraction of N_{ph} excitations seen in Fig. 4 point towards increased correlations which are expected to lead to deformation. The strong presence of N_{ph} excitations from the $\nu 0f_{\frac{7}{2}}$ orbital in $^{46-48}$Ar is a clear manifestation of the strong quadrupole interaction between protons in the *sd* shell and neutrons in the *pf* shell that results in energy gains comparable to the $N = 28$ gap. Some of these N_{ph} excitations are very collective and may produce rapid transitions from spherical to deformed nuclear shapes. The increase of quadrupole collectivity in the heavy Argon and Sulfur isotopes around $N = 28$ is driven by the *sd*-shell valence protons outside the $Z = 14$ sub-shell closure. The relevant orbits, $\pi 1s_{\frac{1}{2}}$ and $\pi 0d_{\frac{3}{2}}$, are known to become degenerate at $N = 28$. This degeneracy maximizes the quadrupole correlation energy of the configurations with open neutron orbits. The Sulfur isotopes with two protons in this pseudo-SU3 space are prolate in this scheme. The ISM calculations for ^{42}S show a well developed γ-band. However, following the criteria of Ref. [3], its γ is found to be small ($5^\circ - 10^\circ$). Calculations for ^{44}S show it to be fully axial whereas ^{46}S develops triaxiality again ($\beta = 0.3$, $\gamma = 20^\circ$). This behavior pertains to variants of Elliott's SU3 coupling scheme; pseudo-SU3 for the protons and quasi-SU3 for the neutrons [20]. The Argon isotopes with two proton-holes in this pseudo-SU3 space are correspondingly oblate, and are found to follow closely the trend of the Sulfur isotopes but with a smaller deformation ($\beta = 0.25$). Using the transition probabilities from the ISM, ^{46}Ar is calculated to be oblate and axial whereas ^{48}Ar is found to be oblate and triaxial with ($\beta = 0.25$, $\gamma = 40^\circ$). The appearance of triaxial shapes can be traced back to the structure of the Nilsson diagrams in this region [21]. At $N = 26$ and $N = 30$ there are two quasi degenerate Nilsson levels available for the last pair of neutrons, both for oblate and prolate deformations. This can induce the K-mixing characteristic of triaxiality. On the contrary, at $N = 28$ deformed gaps develop both in the prolate and oblate sides, making ^{44}S and ^{46}Ar axial.

In summary, new limits of γ spectroscopy of the most neutron rich Ar isotopes at energies around the Coulomb barrier studied with deep inelastic transfer reactions have been presented. Shell model calculations which are in good agreement with the measured energies predict a large fraction of one and two neutron particle-hole excitations across the $N = 28$ shell gap, thus predicting a development of collectivity near a closed shell. The effect of these correlations is manifested by the presence of a triaxial intrinsic structure in ^{48}Ar. The measurements of transition probabilities and the occupancy of the neutron $\nu 0f_{\frac{7}{2}}$ orbital would further confirm the predictions of a non axially symmetric deformation in ^{48}Ar and also in the less accessible ^{46}S. This would increase our understanding of shape evolutions far from the valley of stability and lead us to more conclusive signatures for the presence of non axial deformations. Given the advances in beam intensities and associated detector development this appears to be within reach.

We would like to thank P. Van Isacker for many illuminating discussions. This work has been partly supported by the European Commission under contract 506065 (EURONS/INTAG), the IN2P3 (France)-CICyT (Spain) collaboration agreement and the FPA2007-66060 grant, MEC (Spain).

---

* Permanent address: VECC, 1/AF Bidhan Nagar,Kolkata 700 064, India
† corresponding author: navin@ganil.fr

[1] B. Bastin *et al.*, Phys. Rev. Lett. **99**, 022503 (2007).
[2] A. Gade *et al.*, Phys. Rev. Lett. **99**, 072502 (2007).
[3] A.S. Davydov *et al.*, Nucl. Phys. A **8**, 237 (1958); A.S. Davydov *et al.*, Nucl. Phys. A **20**, 499 (1960).
[4] E. Caurier *et al.*, Nucl. Phys. A **742**, 14 (2004).
[5] D. Sohler *et al.*, Phys. Rev. C **66**, 054302 (2002).
[6] H. Scheit *et al.*, Phys. Rev. Lett. **77**, 3967 (1996).
[7] C.E. Svensson *et al.*, Phys. Rev. Lett. **85**, 2693 (2000).
[8] S. Nummela *et al.*, Phys. Rev. C **63**, 044316 (2001).
[9] B. Jurado *et al.*, Phys. Lett. B **649**, 43 (2007).
[10] L. Gaudefroy*et al.*, Phys. Rev. Lett. **97**, 092501 (2006); A. Signoracci and B. A. Brown Phys. Rev. Lett. **99**, 099201 (2007).
[11] D. Kurath, Phys. Rev. C **5**, 768 (1972).
[12] R. Broda, J. Phys. G **32**, R151 (2006).
[13] M. Rejmund *et al.*, Phys. Rev. C **76**, 021304(R) (2007).
[14] P. Sugathan *et al.*, NIM. **A** (in press).
[15] S. Grevy *et al.*, Phys. Lett. B **594**, 252 (2004).
[16] NDS http://www.nndc.bnl.gov; B. Fornal *et al.*, Eur. Phys. J. **A7**, 147 (2000); L. A. Riley *et al.*, Phys. Rev. C

72, 024311 (2005).
[17] E. Caurier *et al.*, Acta Phys. Pol. B **30**, 705 (1999).
[18] L. Gaudefroy*et al.*, Phys. Rev. Lett. **99**, 099202 (2007).
[19] Zs. Dombradi *et al.*, Nucl. Phys. A **727**, 195 (2003).
[20] A. P. Zuker *et al.*, Phys. Rev. C **52**, R1741 (1995).
[21] E. Caurier *et al.*, Rev. Mod. Phys. 77, 427 (2005).